Finally, we close with a remark on terminology. Although we have not had occasion to do so in this communication, the need will likely arise to refer to a channeled atom (or trajectory) as a particle with a characteristic name. We suggest for this purpose the term *stenon*, from the Greek noun τα στενός, denoting a strait or a mountain pass.[35]

[35] H. G. Liddell and R. Scott, *Greek-English Lexicon* (Oxford University Press, London, 1940), p. 1638.

ACKNOWLEDGMENT

We are particularly grateful to J. A. Davies and G. R. Piercy of Atomic Energy of Canada Ltd., Chalk River, Ontario, for communicating much of their experimental data to us in advance of publication, for permission to reproduce Fig. 17, and for several stimulating and fruitful conversations.

It is a pleasure to acknowledge many valuable discussions with our colleagues C. Lehmann, G. Leibfried, and especially D. K. Holmes.

PHYSICAL REVIEW VOLUME 132, NUMBER 6 15 DECEMBER 1963

Spin-Wave Spectra of Yttrium and Gadolinium Iron Garnet*

A. Brooks Harris
Department of Physics, Duke University, Durham, North Carolina
(Received 13 May 1963)

The problem of deducing the values of the exchange integrals in yttrium and gadolinium iron garnet from measurements of the magnetization and the magnetic contribution to the specific heat at low temperatures is considered. For these garnets the spin-wave normal modes can be found by solving the semiclassical equations of motion which give rise to a set of n simultaneous linear equations, where n is the number of magnetically inequivalent ions in the unit cell. Expressions for the thermodynamic functions at low temperatures in terms of the frequencies of the normal modes are given assuming the validity of the spin-wave approximation. It is argued that the temperature variation of the frequency of these normal modes on the macroscopic properties can be completely accounted for without considering the zero point energy explicitly. Due to the size of the unit cell, the equations for the frequencies of the normal modes can only be solved numerically for general values of $\mathbf{k}$. Such solutions are obtained for $\mathbf{k}$ lying along a [111] direction for various values of the exchange integrals, and the thermodynamic functions corresponding to these choices of parameters are calculated. In the case of yttrium iron garnet, the value of D, the coefficient of a^2k^2 in the acoustic dispersion law, is reliably known and fixes one linear combination of J_{aa}, J_{ad}, and J_{dd}. By comparing our calculations with the magnetization data of Solt, it was established that $J_{aa}/J_{ad}=0.2$, but since the magnetization was not very sensitive to variations of the ratio J_{dd}/J_{ad} its value could not be estimated precisely. Taking $J_{dd}/J_{ad}=0.2$ gives $J_{aa}=J_{dd}=6.35$ cm^{-1} and $J_{ad}=31.8$ cm^{-1}. For GdIG the specific heat data below 20°K is not very much influenced by the exact values of the iron-iron exchange integrals which were taken to be those quoted above for yttrium iron garnet. Again one combination of J_{ac} and J_{dc} is known from the calorimetric determination of the single ion splitting. By comparing the specific heat data below 5°K with calculations for various values of J_{ac}/J_{dc} it was possible to determine J_{ac} and J_{dc} separately: $J_{dc}=7.00$ cm^{-1} and $J_{ac}=1.75$ cm^{-1}. These values are about 25% larger than what one would expect using the Weiss molecular field approximation.

I. INTRODUCTION

RECENTLY many investigations of the behavior of the series of iron garnet compounds have been made. Pauthenet[1] first interpreted their magnetic properties below the Néel point at 550°K using the Weiss molecular field (WMF) approximation. More recently it has been demonstrated[2–5] that at the lowest temperatures one must use the spin-wave approximation in many cases to interpret the thermal and magnetic properties of the iron garnets. The earliest calculations[3,4] gave a value of the excitation energy of the various normal modes (spin waves) for $\mathbf{k}=0$, where $\mathbf{k}$ is a vector of the first Brillouin zone. While this is often sufficient to describe the resonance behavior of the iron garnets, it would seem desirable to make more accurate calculations of the macroscopic properties which take into account the $\mathbf{k}$ dependence of the excitation energies. Tinkham[5] has made such a calculation for a simplified model of the interactions in ytterbium iron garnet (YbIG). He has shown that there are spin-wave modes whose energy is not very dependent on $\mathbf{k}$ and is roughly equal to the energy of the single ion splitting of the rare-earth ion in the WMF approximation, which can be determined calorimetrically.[6] Thus the physical picture of the magnetic behavior of the

* Work carried out with support of the U. S. Office of Naval Research under Contract Nonr 1811(12).
[1] R. Pauthenet, Ann. Phys. **3**, 424 (1958); J. Phys. Radium **20**, 388 (1959).
[2] H. Meyer and A. B. Harris, J. Appl. Phys. **31**, 49S (1960).
[3] R. L. Douglass, Phys. Rev. **120**, 1612 (1960).
[4] B. Dreyfus, J. Phys. Chem. Solids **23**, 287 (1962).
[5] M. Tinkham, Phys. Rev. **124**, 311 (1961).
[6] A. B. Harris and H. Meyer, Phys. Rev. **127**, 101 (1962).

iron garnets can be considered to be well understood. The aim of the present more detailed calculation is twofold. First, it was felt that by making accurate calculations of the spin-wave spectrum for $\mathbf{k}\neq 0$ a more detailed comparison between theory and experiment could be made. Second, it was of interest to see the correspondence in detail between such a complete calculation and other calculations, such as that using the WMF approximation, which do not take full cognizance of the structure of the unit cell.

For yttrium iron garnet (YIG) and gadolinium iron garnet (GdIG) the difficulty in such a calculation arises from the complexity of the unit cell. As is well known, the frequencies of the normal modes of an isotropic spin system can be found by solving the classical equations of motion, which give rise to a secular equation whose degree is in general equal to the number of magnetic ions in the unit cell. A considerable simplification in the numerical calculations is obtained if one assumes that the energy surfaces in k space are spherical. Under this assumption it is only necessary to solve the secular equation for k lying along a [111] direction, in which case the secular equation can be factored. It seems unlikely that this simplification could introduce significant errors into the calculation of the macroscopic properties, because the thermodynamic functions do not depend sensitively on the exact details of the frequency spectrum.

II. CALCULATION OF THE SPIN-WAVE SPECTRUM

A. Lattice Structure

Before calculating the excitation spectrum of spin waves, it is necessary to discuss briefly the lattice structure of the iron garnets. The crystal structure of the iron garnets is cubic, the space group being $O_h^{10}-Ia3d$.[7] The most important symmetry property of the crystal is that the [111] direction is a threefold axis. In Table I we give the positions of the magnetic ions in the unit cell. Each unit cell contains four formula units of iron garnet, $5Fe_2O_3\cdot 3M_2O_3$, where M is yttrium or any of the rare earths from samarium to lutetium. Studies of the magnetic behavior of the garnets[1] show that the iron ions on the a and d sublattices are strongly coupled together antiferromagnetically with a resulting Néel temperature of about 550°K. When rare-earth ions occupy the c sites, their spin moments are coupled antiferromagnetically to the resultant moment of the a and d sublattices. This coupling, which is much weaker and hence does not affect the Néel temperature, produces anomalies in the specific heat and magnetization below 30°K. The magnetic ions are also subjected to a crystalline electric field, which often produces an easy axis of magnetization along a [111] direction.[8,9] For ions which are in an S state, e.g., for Fe^{3+} or Gd^{3+}, the strength of this field corresponds to splittings of the order of 0.01 cm^{-1} or less[8] and hence can be neglected for the present calculations.

TABLE I. The location of the magnetic ions in the unit cell of the garnet lattice.[a]

a sites	d sites	c sites
(1) 0, 0, 0	$0, \frac{1}{4}, \frac{3}{8}$	$0, \frac{1}{4}, \frac{1}{8}$
(2) $\frac{1}{2}, \frac{1}{2}, 0$	$\frac{3}{8}, 0, \frac{1}{4}$	$\frac{1}{8}, 0, \frac{1}{4}$
(3) $0, \frac{1}{2}, \frac{1}{2}$	$\frac{1}{4}, \frac{3}{8}, 0$	$\frac{1}{4}, \frac{1}{8}, 0$
(4) $\frac{1}{2}, 0, \frac{1}{2}$	$0, \frac{3}{4}, \frac{1}{8}$	$0, \frac{3}{4}, \frac{3}{8}$
(5) $\frac{1}{4}, \frac{1}{4}, \frac{1}{4}$	$\frac{1}{8}, 0, \frac{3}{4}$	$\frac{3}{8}, 0, \frac{3}{4}$
(6) $\frac{3}{4}, \frac{1}{4}, \frac{3}{4}$	$\frac{3}{4}, \frac{1}{8}, 0$	$\frac{3}{4}, \frac{3}{8}, 0$
(7) $\frac{3}{4}, \frac{3}{4}, \frac{1}{4}$	$0, \frac{1}{4}, \frac{7}{8}$	$0, \frac{1}{4}, \frac{5}{8}$
(8) $\frac{1}{4}, \frac{3}{4}, \frac{3}{4}$	$\frac{7}{8}, 0, \frac{1}{4}$	$\frac{5}{8}, 0, \frac{1}{4}$
(9)	$\frac{1}{4}, \frac{7}{8}, 0$	$\frac{1}{4}, \frac{5}{8}, 0$
(10)	$0, \frac{3}{4}, \frac{5}{8}$	$0, \frac{3}{4}, \frac{7}{8}$
(11)	$\frac{5}{8}, 0, \frac{3}{4}$	$\frac{7}{8}, 0, \frac{3}{4}$
(12)	$\frac{3}{4}, \frac{5}{8}, 0$	$\frac{3}{4}, \frac{7}{8}, 0$

[a] The coordinates of the magnetic ions are given as fractions of the lattice parameter which is 12.378 Å for YIG and 12.465 Å for GdIG (Ref. 1). The additional sites in the unit cell are obtained by adding $(\frac{1}{4},\frac{1}{4},\frac{1}{4})$ to the above sites. This table is compiled from Ref. 7.

[7] R. Wyckoff, *Crystal Structures* (Interscience Publishers, Inc., New York, 1953), Vol. III, Chap. 12.

B. The Equations of Motion of an Isotropic Spin System

We now treat the case of an isotropic system of interacting spins in an external magnetic field $\mathbf{H}$ for which the Hamiltonian is,

$$\mathcal{H}=-\sum_{rr'} J_{rr'}\mathbf{S}_r\cdot\mathbf{S}_{r'}-\sum_r g_r\beta\mathbf{H}\cdot\mathbf{S}_r, \tag{1}$$

where S_r and g_r are the spin and g value of the ion at $\mathbf{r}$, β is the Bohr magneton, and $J_{rr'}$ is an interaction coefficient. The ions of the three magnetic sublattices are assumed to interact with one another only if they are the closest pair in the sublattices in question. The dipolar interactions correspond to energies which are very much smaller than iron rare-earth exchange energy and hence are taken into account only insofar as their effect is equivalent to that of a demagnetizing field which can be included in $\mathbf{H}$. Semiclassically one uses the torque equation to determine the frequencies of the normal modes

$$d\mathbf{S}_r/dt=\gamma_r(\mathbf{S}_r\times\mathbf{H}_r) \tag{2a}$$

$$d\mathbf{S}_r/dt=\mathbf{S}_r\times[(1/\hbar)(\sum_{r'} 2J_{rr'}\mathbf{S}_{r'})+\gamma_r\mathbf{H}], \tag{2b}$$

where γ_r is the gyromagnetic ratio of the ion at $\mathbf{r}$. Quantum mechanically, the equations of motion are

$$\langle n|[\mathcal{H},S_r^+]|m\rangle=\hbar\omega\langle n|S_r^+|m\rangle \tag{3a}$$

and

$$\langle n|[\mathcal{H},S_r^-]|m\rangle=-\hbar\omega\langle n|S_r^-|m\rangle, \tag{3b}$$

[8] G. P. Rodrigue, H. Meyer, and R. V. Jones, J. Appl. Phys. **31**, 376S (1960).

[9] R. F. Pearson and R. W. Cooper, J. Phys. Soc. Japan **17**, Suppl. B1, 369 (1962).

$$\begin{matrix} A_{aa}^{T}(k) & A_{ad}^{*}(k) \\ -A_{ad}^{T}(k) & -A_{dd}(-k) \end{matrix}$$

FIG. 1. The form of the spin-wave matrix, A_{ij}, for YIG. The submatrices are given in Figs. 3–7.

where $S_r^{\pm}=S_r^x\pm iS_r^y$. One finds, using Eq. (1) and the commutation relations, $\mathbf{S}\times\mathbf{S}=i\mathbf{S}$, that

$$[\mathcal{H},S_r^+]=g_r\beta HS_r^+-2\sum_{r'}J_{rr'}(S_r^+S_{r'}^z-S_r^zS_{r'}^+) \quad (4a)$$

and

$$[\mathcal{H},S_r^-]=-g_r\beta HS_r^-+2\sum_{r'}J_{rr'}(S_r^-S_{r'}^z-S_r^zS_{r'}^-), \quad (4b)$$

if the magnetic field is oriented in the minus z direction. In the random phase approximation (RPA)[10] one replaces the operator S_r^z by its thermal value, $\langle S_r^z\rangle$.[11] This corresponds exactly to linearizing the semiclassical equations of motion.

In either case if one writes

$$S_{\mathbf{k}r}^+=(2N_{uc})^{-1/2}\sum_{\mathbf{R}}S_{\mathbf{R}+r}^+e^{i\mathbf{k}\cdot(\mathbf{R}+r)},$$

where r denotes the position of an ion in the unit cell, $\mathbf{R}$ is a translation vector of the lattice (which we take to be body-centered cubic), $\mathbf{k}$ is a vector in the first

$$\begin{matrix} A_{aa}^{T}(k) & A_{ad}^{*}(k) & A_{ac}^{*}(k) \\ -A_{ad}^{T}(k) & -A_{dd}(-k) & -A_{cd}^{T}(-k) \\ A_{ac}^{T}(k) & A_{cd}^{*}(-k) & \Delta\,\underline{1} \end{matrix}$$

FIG. 2. The form of the spin-wave matrix, A_{ij}, for GdIG. $\mathbf{1}$ is the unit matrix and $\Delta=-10J_{dc}+20J_{ac}$. The submatrices are given in Figs. 3–7.

Brillouin zone, and N_{uc} is the number of unit cells, then one finds[6] that for each value of $\mathbf{k}$ the allowed values of $\hbar\omega$ are the eigenvalues of the matrix $\mathbf{A}$, whose components are

$$A_{ij}=[g_i\beta H-2\sum_{j'}J_{ij'}S_{j'}{}^z\gamma_{ij'}(0)]\delta_{ij}+2J_{ij}(S_j/S_i)^{1/2}S_i{}^z\gamma_{ij}(\mathbf{k}), \quad (5)$$

where the indices i and j label the ions in the unit cell, and $\gamma_{ij}=\sum_{j'}e^{i\mathbf{k}\cdot(\mathbf{r}_i-\mathbf{r}_{j'})}$, the sum being taken over nearest neighboring ions in the jth sublattice. The dimensionality of this matrix is equal to the number of magnetic sublattices, i.e., 20 for YIG and 32 for GdIG.

$$\begin{matrix} A_1 & 0 & 0 & 0 & A_3 & A_2 & A_2 & A_2 \\ 0 & A_1 & 0 & 0 & A_2 & A_2 & A_3 & A_2 \\ 0 & 0 & A_1 & 0 & A_2 & A_2 & A_2 & A_3 \\ 0 & 0 & 0 & A_1 & A_2 & A_3 & A_2 & A_2 \\ A_3 & A_2 & A_2 & A_2 & A_1 & 0 & 0 & 0 \\ A_2 & A_2 & A_2 & A_3 & 0 & A_1 & 0 & 0 \\ A_2 & A_3 & A_2 & A_2 & 0 & 0 & A_1 & 0 \\ A_2 & A_2 & A_3 & A_2 & 0 & 0 & 0 & A_2 \end{matrix}$$

FIG. 3. The submatrix $A_{aa}(k)$. Here $A_1=-30J_{ad}+40J_{aa}+12J_{ac}S_c$, $A_2=-10J_{aa}\cos(ka/4)$, and $A_3=-10J_{aa}\cos(3ka/4)$. Here and in Figs. 4–9 we use the notation $k_x=k_y=k_z=k$.

[10] F. Englert, Phys. Rev. Letters **5**, 102 (1960).

[11] The excitation energies calculated using the thermal value of S_r^z are not exactly those one should use in the calculations of the thermodynamic functions (see the Appendix).

These matrices are shown in Figs. 1 and 2, where the sublattices are given in Figs. 3–7. The numbering of the rows and columns of A_{ij} correspond to the numbering of the magnetic ions as given in Table I.

$$\begin{matrix} 0 & 0 & 0 & M_1 & M_1 & M_1 & M_1^* & M_1^* & M_1^* & 0 & 0 & 0 \\ M_1^* & 0 & M_2 & 0 & M_2^* & 0 & 0 & M_2 & 0 & M_1 & 0 & M_2^* \\ M_2 & M_1^* & 0 & 0 & 0 & M_2^* & 0 & 0 & M_2 & M_2^* & M_1 & 0 \\ 0 & M_2 & M_1^* & M_2^* & 0 & 0 & M_2 & 0 & 0 & 0 & M_2^* & M_1 \\ M_1 & M_1 & M_1 & 0 & 0 & 0 & 0 & 0 & 0 & M_1^* & M_1^* & M_1^* \\ 0 & M_2^* & 0 & M_2 & 0 & M_1^* & M_2^* & 0 & M_1 & 0 & M_2 & 0 \\ 0 & 0 & M_2^* & M_1^* & M_2 & 0 & M_1 & M_2^* & 0 & 0 & 0 & M_2 \\ M_2^* & 0 & 0 & 0 & M_1^* & M_2 & 0 & M_1 & M_2^* & M_2 & 0 & 0 \end{matrix}$$

FIG. 4. The submatrix $A_{ad}(k)$. Here $M_1=-5J_{ad}\exp(ika/8)$ and $M_2=-5J_{ad}\exp(3ika/8)$.

Let us consider some general properties of this matrix A_{ij}. It can be transformed into the form,

$$\begin{pmatrix} \mathbf{B} & \mathbf{C} \\ -\mathbf{C}^{*T} & \mathbf{D} \end{pmatrix}, \quad (6)$$

where $\mathbf{D}$ and $\mathbf{B}$ are Hermitian submatrices, and the

$$\begin{matrix} D & 0 & 0 & 0 & 0 & 0 & 0 & D_3 & D_1 & 0 & D_2^* & D_2^* \\ 0 & D & 0 & 0 & 0 & 0 & D_1 & 0 & D_3 & D_2^* & 0 & D_2^* \\ 0 & 0 & D & 0 & 0 & 0 & D_3 & D_1 & 0 & D_2^* & D_2^* & 0 \\ 0 & 0 & 0 & D & 0 & 0 & 0 & D_2^* & D_2^* & 0 & D_1 & D_3 \\ 0 & 0 & 0 & 0 & D & 0 & D_2^* & 0 & D_2^* & D_3 & 0 & D_1 \\ 0 & 0 & 0 & 0 & 0 & D & D_2^* & D_2^* & 0 & D_1 & D_3 & 0 \\ 0 & D_1 & D_3^* & 0 & D_2 & D_2 & D & 0 & 0 & 0 & 0 & 0 \\ D_3^* & 0 & D_1 & D_2 & 0 & D_2 & 0 & D & 0 & 0 & 0 & 0 \\ D_1 & D_3^* & 0 & D_2 & D_2 & 0 & 0 & 0 & D & 0 & 0 & 0 \\ 0 & D_2 & D_2 & 0 & D_3^* & D_1 & 0 & 0 & 0 & D & 0 & 0 \\ D_2 & 0 & D_2 & D_1 & 0 & D_3^* & 0 & 0 & 0 & 0 & D & 0 \\ D_2 & D_2 & 0 & D_3^* & D_1 & 0 & 0 & 0 & 0 & 0 & 0 & D \end{matrix}$$

FIG. 5. The submatrix $A_{dd}(k)$. Here
$D=-20J_{ad}+20J_{dd}-4J_{cd}S_c$,
$D_1=-5J_{dd}$,
$D_2=-5J_{dd}\exp(ika/4)$,
$D_3=-5J_{dd}\exp(ika/2)$.

superscript T represents the transpose. To diagonalize $\mathbf{A}$, we look for a matrix $\mathbf{O}$ such that

$$\mathbf{O}^\dagger\mathbf{A}\mathbf{O}=\mathbf{A}_d, \quad (7)$$

where $\mathbf{A}_d$ is diagonal, and where, due to the form of $\mathbf{A}$, $\mathbf{O}$, and $\mathbf{O}^\dagger$ satisfy the conditions

$$\mathbf{O}^\dagger\mathbf{O}=\mathbf{1}, \quad \mathbf{O}=\begin{pmatrix} \mathbf{O}_{11} & \mathbf{O}_{12} \\ \mathbf{O}_{21} & \mathbf{O}_{22} \end{pmatrix},$$

$$\mathbf{O}^\dagger=\begin{pmatrix} \mathbf{O}_{11}{}^{*T} & -\mathbf{O}_{21}{}^{*T} \\ -\mathbf{O}_{12}{}^{*T} & \mathbf{O}_{22}{}^{*T} \end{pmatrix}, \quad (8)$$

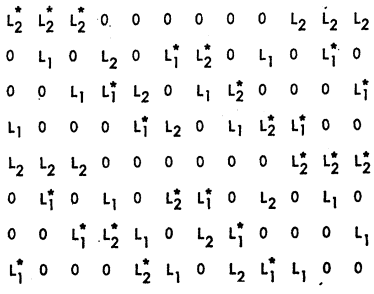

FIG. 6. The submatrix $A_{ac}(k)$. Here $L_1=-2(5S_c/2)^{1/2}J_{ac}\times\exp(ika/8)$, $L_2=-2(5S_c/2)^{1/2}J_{ac}\times\exp(3ika/8)$.

where the $\mathbf{O}_{ij}$ are suitable submatrices. Since $\mathbf{A}$ is not Hermitian, the roots need not be real, but, as indicated by Douglass,[3] this would imply an unstable ground configuration. In terms of the occupation numbers $n_{\rho\mathbf{k}}$, the energy levels of the spin system are approximately

$$E=E^{00}+\sum_{\rho\mathbf{k}} n_{\rho\mathbf{k}}|\hbar\omega_{\rho\mathbf{k}}|\,, \tag{9}$$

where ρ labels the branch of the spectrum and E^{00} is the ground-state energy.[12]

Let us now calculate $\mu_{\rho\mathbf{k}}$, the change in the magnetic moment when $n_{\rho\mathbf{k}}$ is increased by one, remembering that the magnetic moment of a state is given by the derivative with respect to the magnetic field of the energy of that state.[13] Then

$$\mu_{\rho\mathbf{k}}=(d/dH)[(n_{\rho\mathbf{k}}+1)|\hbar\omega_{\rho\mathbf{k}}|-n_{\rho\mathbf{k}}|\hbar\omega_{\rho\mathbf{k}}|] \tag{10a}$$

$$=(d/dH)|\hbar\omega_{\rho\mathbf{k}}|=\sigma_\rho(d/dH)\hbar\omega_{\rho\mathbf{k}}\,, \tag{10b}$$

where σ_ρ, the polarization of the ρth mode, is just the sign of $\hbar\omega_{\rho\mathbf{k}}$. Using perturbation theory one finds

$$\mu_{\rho\mathbf{k}}=\sigma_\rho\{\mathbf{O}^\dagger[d\mathbf{A}(\mathbf{k})/dH]\mathbf{O}\}_{\rho\rho}=\sigma_\rho\beta(\mathbf{O}^\dagger\mathbf{G}\mathbf{O})_{\rho\rho}\,, \tag{11}$$

where $\mathbf{G}$ is diagonal and G_{mm} is the g value of the mth ion in the unit cell. When all the g values are the same, as for YIG and GdIG, one has the simple result that

$$\mu_{\rho\mathbf{k}}=\sigma_\rho\beta g\,. \tag{12}$$

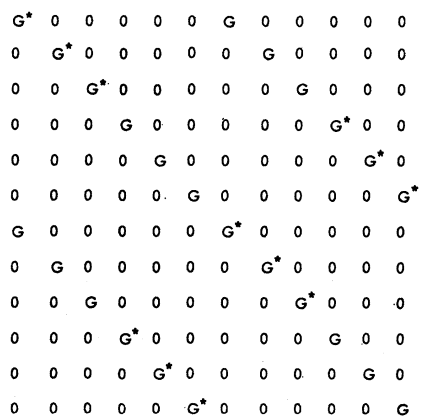

FIG. 7. The submatrix $A_{cd}(k)$. Here $G=-2(5S_c/2)^{1/2}J_{cd}\exp(ika/4)$.

We now consider some properties of the solution to this eigenvalue problem taking account of the symmetry of the garnet lattice. For $\mathbf{k}=0$, the symmetry is sufficient to permit a factorization of the secular determinant and thence a complete analytic determination when k lies along a [111] direction, which we assume to be the case in the following discussion. We denote by $\mathbf{R}$ the operator which rotates the crystal about the [111] direction by $\frac{2}{3}\pi$. We note that since $\mathbf{R}$ commutes with $\mathbf{A}$,

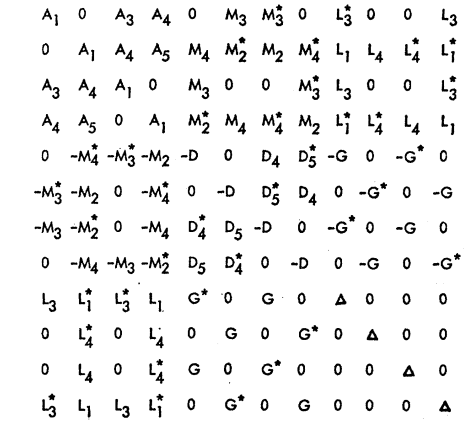

FIG. 8. The transformed spin-wave matrix of Eq. (13), $A(k,1)$. For GdIG the entire matrix is solved. For YIG one solves the 8×8 matrix obtained by deleting the right-hand four columns and the bottom four rows. The symbols not defined in the captions of previous figures are $A_4=\sqrt{3}A_2$, $A_5=2A_2+A_3$, $M_3=\sqrt{3}M_1$, $M_4=M_1{}^*+M_2$, $L_3=\sqrt{3}L_2$, $L_4=L_1{}^*+L_2$, $D_4=-D_1-D_3$, and $D_5=-2D_2$.

the eigenvectors of $\mathbf{A}$ are also eigenvectors of $\mathbf{R}$. Since $\mathbf{R}^3=1$, the eigenvalues of $\mathbf{R}$ are just the cube roots of unity, 1, λ, and λ^2, where $\lambda=\exp(2\pi i/3)$. The secular equation may then be written in the form,

$$\mathrm{Det}|\mathbf{A}(\mathbf{k},1)-\hbar\omega_{\mathbf{k},1}||\mathbf{A}(\mathbf{k},\lambda)-\hbar\omega_{\mathbf{k},\lambda}||\mathbf{A}(\mathbf{k},\lambda^2)-\hbar\omega_{\mathbf{k},\lambda^2}|=0\,, \tag{13}$$

where the eigenvectors of $\mathbf{A}(\mathbf{k},r)$ are associated with the eigenvalue r of $\mathbf{R}$. These matrices are given in Figs. 8 and 9, and in Table II we give the linear combinations of rows and columns of $\mathbf{A}$ which correspond to the rows and columns of $\mathbf{A}(\mathbf{k},r)$. Using Fig. 9, one verifies that

$$\mathbf{P}^{-1}\mathbf{A}(\mathbf{k},\lambda)\mathbf{P}=\mathbf{A}(-\mathbf{k},\lambda)=\mathbf{A}^*(\mathbf{k},\lambda^2)\,, \tag{14}$$

where $\mathbf{P}$ is a unitary transformation which interchanges rows and columns as follows: $3\rightleftarrows6$, $4\rightleftarrows5$, $7\rightleftarrows10$, $8\rightleftarrows9$. Since the frequencies are assumed to be real, $\mathbf{A}(\mathbf{k},\lambda)$ and $\mathbf{A}(\mathbf{k},\lambda^2)$ have the same eigenvalues.

Although the secular equation factors, analytic solutions are obtainable only at the center or extreme corner of the Brillouin zone.[3,4] However, since the magnetic properties at the lowest temperatures depend only on the behavior of the low-energy part of the

[12] In the Appendix we show that the temperature dependence of the frequencies of the normal modes does not affect the zero point energy.

[13] J. H. Van Vleck, *Theory of Electric and Magnetic Susceptibilities* (Oxford University Press, New York, 1932).

A_1	A_6	M_5	M_6	$\bar{M}_6$	M_7	L_5	L_6	L_7	L_5
A_6^*	A_1	M_6	M_8	M_9	$\bar{M}_6$	$\bar{L}_5$	L_8	L_9	L_5
$-M_5^*$	$-M_6^*$	$-D$	0	D_6	D_2^*	$-G$	0	$-G^*$	0
$-M_6^*$	$-M_8^*$	0	$-D$	D_2^*	D_7	0	$-G^*$	0	$-G$
$-\bar{M}_6^*$	$-M_9^*$	D_6^*	D_2	$-D$	0	$-G^*$	0	$-G$	0
$-M_7^*$	$-\bar{M}_6^*$	D_2	D_7^*	0	$-D$	0	$-G$	0	$-G^*$
L_5^*	$\bar{L}_5^*$	G^*	0	G	0	Δ	0	0	0
L_6^*	L_8^*	0	G	0	G^*	0	Δ	0	0
L_7^*	L_9^*	G	0	G^*	0	0	0	Δ	0
$\bar{L}_5^*$	L_5^*	0	G^*	0	G	0	0	0	Δ

FIG. 9. The transformed spin-wave matrix of Eq. (13), $A(k,\lambda)$. For GdIG the entire matrix is solved. For YIG one solves the 6×6 matrix obtained by deleting the right-hand four columns and the bottom four rows. The symbols not defined in the captions of previous figures are $A_6=\lambda(A_3-A_2)$, $M_5=M_1{}^*+\lambda^2M_2$, $M_6=\lambda M_2$, $M_6=\lambda M_2{}^*$, $M_7=M_1+\lambda^2M_2{}^*$, $M_8=M_2+\lambda^2M_1{}^*$, $M_9=M_2{}^*+\lambda^2M_1$, $L_5=\lambda L_1$, $\bar{L}_5=\lambda L_1{}^*$, $L_6=L_2+\lambda^2L_1{}^*$, $L_7=L_2{}^*+\lambda^2L_1$, $L_8=L_1+\lambda^2L_2{}^*$, $L_9=L_1{}^*+\lambda^2L_2$, and $D_7=-\lambda D_3-\lambda^2D_1$.

spectrum it may be useful to expand the energy of the acoustic branch in powers of k. Due to the cubic symmetry this expansion takes the form

$$\hbar\omega=g\beta H+Da^2k^2+Ea^4k^4+Fa^4(k_x{}^2k_y{}^2+k_x{}^2k_z{}^2+k_y{}^2k_z{}^2)+\cdots. \quad (15)$$

By perturbation methods one finds[4]

$$D=\frac{200J_{aa}-125J_{ad}+75J_{dd}-20J_{dc}S_c+50J_{ac}S_c}{16(-5+6S_c)}. \quad (16)$$

For YIG ($S_c=0$) one also finds

$$E=\frac{5}{12\,288}\left[(32J_{aa}-19J_{ad}+12J_{dd})-\frac{(48J_{aa}-25J_{ad}+12J_{dd})^2}{J_{ad}}\right], \quad (17)$$

TABLE II. The transformation which reduces the spin-wave matrix.[a]

For $\mathbf{A}(\mathbf{k},1)$	For $\mathbf{A}(\mathbf{k},\lambda)$[b]
(1) a_1	
(2) $(1/\sqrt{3})(a_2+a_3+a_4)$	(1) $(1/\sqrt{3})(a_2+\lambda a_3+\lambda^2a_4)$
(3) a_5	
(4) $(1/\sqrt{3})(a_6+a_7+a_8)$	(2) $(1/\sqrt{3})(a_6+\lambda a_7+\lambda^2a_8)$
(5) $(1/\sqrt{3})(d_1+d_2+d_3)$	(3) $(1/\sqrt{3})(d_1+\lambda d_2+\lambda^2d_3)$
(6) $(1/\sqrt{3})(d_4+d_5+d_6)$	(4) $(1/\sqrt{3})(d_4+\lambda d_5+\lambda^2d_6)$
(7) $(1/\sqrt{3})(d_7+d_8+d_9)$	(5) $(1/\sqrt{3})(d_7+\lambda d_8+\lambda^2d_9)$
(8) $(1/\sqrt{3})(d_{10}+d_{11}+d_{12})$	(6) $(1/\sqrt{3})(d_{10}+\lambda d_{11}+\lambda^2d_{12})$
(9) $(1/\sqrt{3})(c_1+c_2+c_3)$	(7) $(1/\sqrt{3})(c_1+\lambda c_2+\lambda^2c_3)$
(10) $(1/\sqrt{3})(c_4+c_5+c_6)$	(8) $(1/\sqrt{3})(c_4+\lambda c_5+\lambda^2c_6)$
(11) $(1/\sqrt{3})(c_7+c_8+c_9)$	(9) $(1/\sqrt{3})(c_7+\lambda c_8+\lambda^2c_9)$
(12) $(1/\sqrt{3})(c_{10}+c_{11}+c_{12})$	(10) $(1/\sqrt{3})(c_{10}+\lambda c_{11}+\lambda^2c_{12})$

[a] The rows and columns of the matrices $\mathbf{A}(\mathbf{k},1)$ and $\mathbf{A}(\mathbf{k},\lambda)$ are labeled by numbers. The rows and columns of the original matrix are labeled by a letter and a number. The letter tells the sublattice and the numbering within the sublattice is according to Table I.

[b] The linear combinations for $\mathbf{A}(\mathbf{k},\lambda^2)$ are found by substituting λ^2 for λ everywhere.

$$F=\frac{5}{12\,288}\left[(128J_{aa}+16J_{ad})+\frac{96J_{ad}{}^2}{8J_{aa}-6J_{ad}}\right]. \quad (18)$$

For GdIG the expressions for E and F are somewhat unwieldy and hence it may be more revealing to give approximate expressions:

$$E=\frac{-6S_cD^2}{\Delta(-5+6S_c)}+\frac{5}{12\,288(-5+6S_c)}\left[-160J_{aa}+95J_{ad}-60J_{dd}+\frac{5(48J_{aa}-25J_{ad}+12J_{dd})^2}{J_{ad}}\right], \quad (19)$$

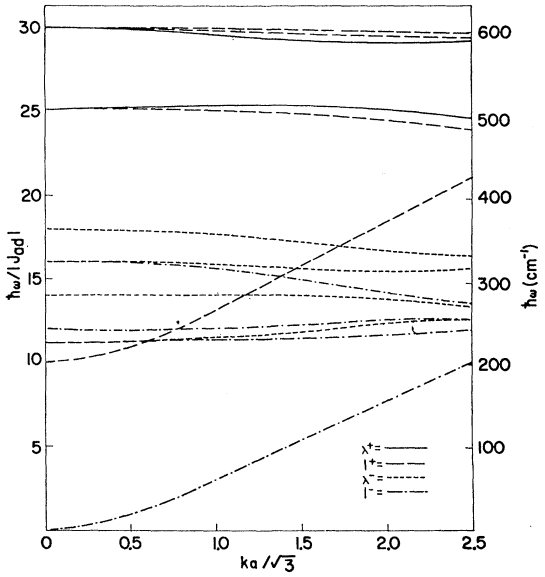

FIG. 10. The spin-wave spectrum for YIG for $\mathbf{k}$ lying along a [111] direction, and for $J_{aa}/J_{ad}=0$ and $J_{dd}/J_{ad}=0.2$ which corresponds to $J_{ad}=20.2$ cm^{-1}. Here and in the following figures the polarization of the mode is indicated by a plus or minus sign. The eigenvalue of the rotation operator is also given. The modes corresponding to the eigenvalues λ and λ^2 are degenerate.

$$F=\frac{5}{12\,288(-5+6S_c)}\left[-640J_{aa}-80J_{aa}+\frac{240J_{ad}{}^2}{3J_{ad}-4J_{aa}}\right], \quad (20)$$

where $\Delta=-10J_{dc}+20J_{ac}$ which is the energy-level splitting of the rare-earth ion in the WMF approximation. For GdIG the term in Eq. (15) involving F is much less important than that involving E, which can usually be adequately approximated by the first term of Eq. (19).

Several observations about these expansions should be made. One sees that the first anisotropic term is that involving F, which vanishes for $J_{aa}=J_{dd}=0$. In any event, one sees that ratio F/E is small for reasonable values of the other exchange integrals, in agreement with our assumption that the energy surfaces in $\mathbf{k}$ space

are nearly spherical. One also notes that E has the opposite sign from D since all the exchange integrals are taken to be negative, with J_{ad} by far the largest. It is interesting to note the role by the spin of the rare-earth ions, S_c. It enters all the expressions in the denominator via a factor $(-5+6S_c)$, thus profoundly affecting D and hence the low-temperature properties. The condition for antiferromagnetism is just $-5+6S_c=0$, in which case our expressions are no longer valid.

In order to discuss the magnetic properties at higher temperature, it is necessary to solve for the normal modes numerically, which necessitated the use of an electronic computer, considering the size of the matrices involved. We used a method of successive approximations: we eliminated the largest off-diagonal element A_{mn} by performing successive two-dimensional rotations,

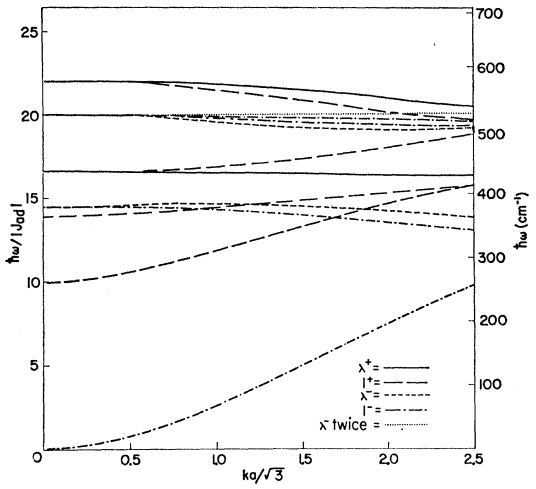

FIG. 11. The spin-wave spectrum for YIG for **k** lying along a [111] direction, and for $J_{aa}/J_{ad}=0.2$ and $J_{dd}/J_{ad}=0$, or $J_{ad}=26.2$ cm^{-1}, $J_{aa}=5.24$ cm^{-1}, and $J_{dd}=0$.

i.e., by performing transformations with a matrix $\mathbf{O}$ obeying Eq. (10) and of the form,

$$O_{ij}=\delta_{ij} \quad i\neq n,m \qquad j\neq n,m \tag{21a}$$

$$O_{nj}=0 \quad j\neq n,m \quad O_{mj}=0 \quad j\neq n,m. \tag{21b}$$

The numerical errors incurred in these calculations were negligible, as was verified by comparing the trace of the original matrix with the sum of the eigenvalues. In addition, for $\mathbf{k}=0$, we found agreement between our numerical results and the analytic expressions of Dreyfus.[4]

The results of calculations for various values of the ratios J_{aa}/J_{ad} and J_{dd}/J_{ad} for the case of YIG are given in Figs. 10, 11, and 12. In Sec. IV we discuss the determination of J_{ad} for given values of these ratios. The most striking feature of the spectrum is that the frequency of most of the modes does not depend strongly on **k**. We can compare the frequencies with those one

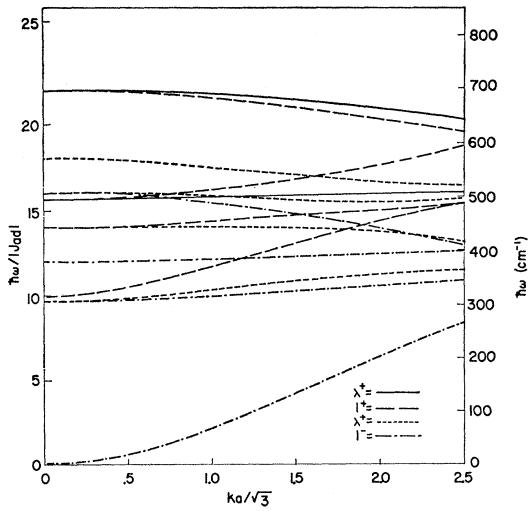

FIG. 12. The spin-wave spectrum for YIG for **k** lying along a [111] direction, and for $J_{aa}/J_{ad}=J_{dd}/J_{ad}=0.2$, or $J_{ad}=31.8$ cm^{-1} and $J_{aa}=J_{dd}=6.35$ cm^{-1}.

would expect using the WMF model. Here one would have eight iron ions on a sites in an effective field H_a, where

$$g\beta H_a=-30J_{ad}+40J_{aa} \tag{22a}$$

and 12 iron ions on d sites in an effective field, H_d, where

$$g\beta H_d=-20J_{ad}+20J_{dd}. \tag{22b}$$

From the graphs one sees that on the whole the frequencies lie somewhat below those of the WMF model

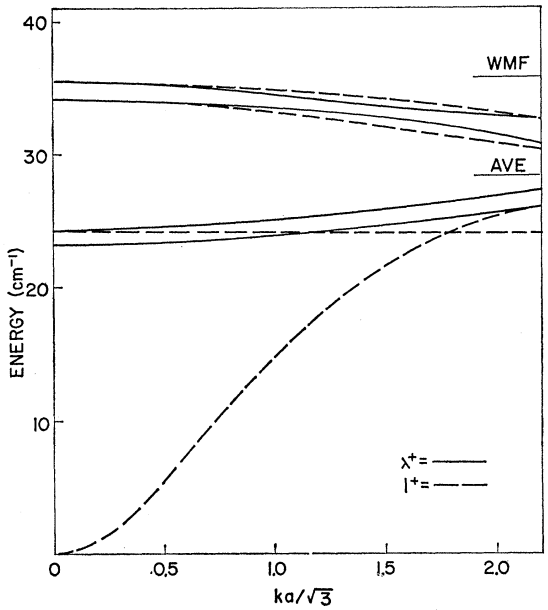

FIG. 13. The low-frequency part of the spin-wave spectrum of GdIG for **k** lying along a [111] direction, and for $J_{ad}=31.8$ cm^{-1} $J_{aa}=J_{dd}=6.35$ cm^{-1}, and $J_{ac}/J_{dc}=0.25$, or $J_{dc}=7.00$ cm^{-1} and $J_{ac}=1.75$ cm^{-1}. See the text for a discussion of the WMF and average frequencies.

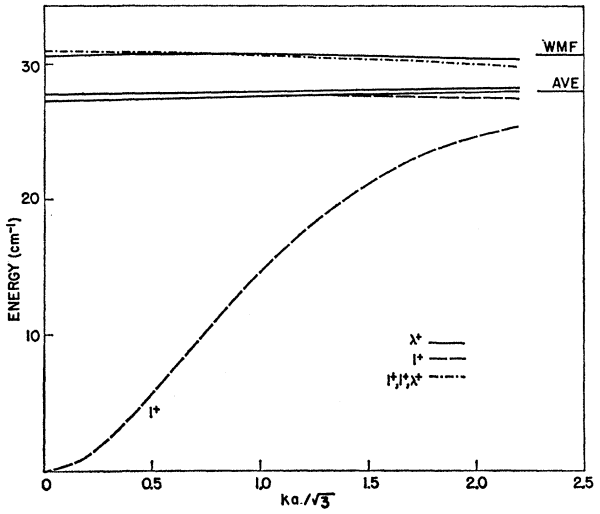

FIG. 14. The low-frequency part of the spin-wave spectrum of GdIG for $\mathbf{k}$ lying along [111] direction, and for $J_{ad}=31.8$ cm^{-1}, $J_{aa}=J_{dd}=6.35$ cm^{-1}, and $J_{ac}/J_{dc}=0.0833$, or $J_{dc}=3.66$ cm^{-1} and $J_{ac}=0.305$ cm^{-1}. For this choice of parameters it happened that one mode was highly degenerate corresponding to eigenvalues of the rotation operator indicated in the legend.

and hence the values of the exchange integrals as deduced from comparison of experimental data with the WMF theory are expected to be less than those we find. This discrepancy is the most serious at the lowest temperatures, just where precise magnetization data is available.

In Fig. 13 and 14 we show the low-frequency part of the spectrum for GdIG for $\mathbf{k}$ lying along a [111] direction. These low optical modes correspond in the WMF picture to the reversal of a Gd^{3+} spin in the effective magnetic field of the iron ions. The high-frequency part of the spectrum is not very different from that of YIG.[14] We have selected values of J_{ac} and J_{dc} such that the average[15] frequency of the low optical modes is that determined calorimetrically.[6] Figures 13 and 14 therefore show the effect on the spectrum of varying the ratio J_{ac}/J_{dc} keeping the average of the low optical frequencies constant. For a given value of this average frequency varying the iron-iron exchange integrals has relatively little effect on the low-frequency part of the spectrum. In contrast, as the ratio J_{ac}/J_{dc} is increased, the low optical modes are split apart and the average frequency becomes significantly less than the WMF splitting which is given by

$$g\beta H_c=-10J_{dc}+20J_{ac}. \tag{23}$$

These results agree with the analytic expressions found by Dreyfus[4] for $\mathbf{k}=0$, which show that the spread in the low optical modes is roughly proportional to $J_{RE}^2S_c$ where J_{RE} is an iron-rare-earth exchange integral.

III. CALCULATION OF THE MACROSCOPIC PROPERTIES

Once the spin-wave spectrum has been found, the magnetization and the specific heat are easily calculated.[16] For instance, for the magnetization one has

$$M(T)=M(0)-\frac{1}{8\pi^3}\sum_n\int_{\text{B.Z.}}\mu_n(\mathbf{k})\times\frac{1}{1-\exp[-x_n(\mathbf{k})]}d\mathbf{k}, \tag{24}$$

where the sum is taken over the normal modes n, the integration over the Brillouin zone, $\mu_n(\mathbf{k})$ is given by Eq. (11) and $x_n(\mathbf{k})=\hbar\omega_n(\mathbf{k})/k_BT$, where k_B is the Boltzmann constant. In order to calculate $M(T)$ from the spectrum as determined for $\mathbf{k}$ lying along a [111] direction, we assumed spherical energy surfaces and integrate over a sphere of radius $k_{\max}$ such that $4\pi k_{\max}^3/3=2(2\pi/a)^3$ since there are two ions per unit cell. Therefore

$$M(T)=M(0)-\frac{1}{8\pi^3}\sum_n\int_0^{k_{\max}}\mu_n(k)\times\frac{1}{1-\exp[-x_n(k)]}4\pi k^2dk. \tag{25}$$

For YIG and GdIG where all the ions have the same g value, one can calculate the magnetization at low temperature when the expansion of Eq. (15) is valid:

$$\Delta M=M(0)-M(T)=\frac{M(0)}{S_{\text{tot}}}\left(\frac{k_BT}{4\pi D}\right)^{3/2}\times\left[\zeta\left(\frac{3}{2}\right)-\frac{3}{4}\zeta\left(\frac{5}{2}\right)\frac{k_BT}{D}\left(\frac{5E+F}{D}\right)\right], \tag{26}$$

where S_{tot} is the total spin per unit cell, i.e., $S_{\text{tot}}=20$ for YIG, and $S_{\text{tot}}=32$ for GdIG. In an analogous way, one finds the specific heat to be

$$C=k_B\frac{V}{8\pi^3}\sum_n\int_0^{k_{\max}}[x_n(k)]^2\times\frac{\exp[-x_n(k)]}{\{1-\exp[-x_n(k)]\}^2}4\pi k^2dk, \tag{27}$$

[14] For small values of k the acoustic branch of the spectra of YIG and GdIG may be thought of as corresponding to one another. The additional 12 normal modes for GdIG are the other 11 low optical modes shown and also another low optical mode for which $\hbar\omega\approx(-5+6S_c)\Delta/5\approx16\Delta/5$. For large values of k the frequency of this latter mode approaches that of the acoustic mode of YIG, whereas the frequency of the acoustic mode of GdIG approaches that of the other 11 low optical modes. This is an example of the principle of noncrossing of eigenvalues.

[15] Calorimetrically one determines a weighted average of the low optical frequencies according to Eq. (27) which, however, is not very different above, say, 10°K from the arithmetic average of these frequencies.

[16] J. Van Kranendonk and J. H. Van Vleck, Rev. Mod. Phys. **30**, 1 (1958).

where V is the volume. Again in zero applied field one can calculate the specific heat when the expansion of Eq. (15) is valid:

$$C=\frac{Vk_B}{a^3}\frac{15}{32}\left(\frac{k_BT}{D\pi}\right)^{3/2}\left[\zeta\left(\frac{5}{2}\right)-\frac{7}{4}\zeta\left(\frac{7}{2}\right)\frac{k_BT}{D}\left(\frac{5E+F}{D}\right)\right]. \quad (28)$$

Expansions for the case when there is an applied field have been given by Robinson[17] assuming a quadratic dispersion relation. From his graphs one can see the relatively large effect of a magnetic field on the magnetization.

It is interesting to consider the range of validity of the expressions (26) and (28). Taking $\Delta/J_{ad}=1$, $J_{aa}/J_{ad}=0.2$, and $J_{dd}/J_{ad}=0.3$, in rough accord with experimental data, one finds using Eqs. (16), (17), and (19) that $E/D=0.31$ for GdIG and 0.12 for YIG. Using Eq. (27) we find a 10% deviation from pure $T^{3/2}$ behavior for the specific heat when $k_BT\approx D/8$ for YIG and $k_BT\approx 0.04D$ for GdIG. Since D/k_B is 45°K for YIG and 15°K for GdIG, one sees that whereas YIG exhibits $T^{3/2}$ behavior below say 6°K, GdIG may never really obey a $T^{3/2}$ law since below 1°K anisotropy and dipolar perturbations will influence the thermal properties.[18]

We now estimate the effect of the temperature dependence on our calculations. In the Appendix we show that at low temperatures one should use the average frequencies, $\hbar\bar{\omega}$, to calculate the thermodynamic functions where

$$\hbar\bar{\omega}(T)=[\hbar\omega(0)+\hbar\omega(T)]/2. \quad (29)$$

To calculate $\hbar\omega(T)$ one simply replaces S_i^z by its thermal value; however, for the iron ions below, say, 50°K the thermal value does not differ appreciably from the value at $T=0$°K. In Table III we compare the frequencies of the normal modes, $\hbar\bar{\omega}$, calculated for $T=0$°K with those calculated for $T=20$°K. The small temperature variation of those frequencies is not experimentally detectible at present. It is interesting to note the increase in the frequencies of the low optical modes as the temperature is raised and the RPA and the WMF become equivalent. This effect results from the change in the effective field acting on the *iron* ions due to the slight temperature dependence of the rare-earth magnetization below 20°K, and is not to be confused with the effect of rare-earth-rare-earth interactions, or with the effect of the temperature dependence of the iron sublattice magnetization both of which we have neglected.

TABLE III. Temperature dependence of the frequencies of the normal modes of GdIG.[a]

	$r=1$		$r=\lambda$	
	$T=0$°K	$T=20$°K	$T=0$°K	$T=20$°K
(1)	19.733	19.811	19.733	19.811
(2)	9.012	9.054	13.561	13.634
(3)	− 3.307	− 3.164	−18.741	−18.645
(4)	−15.083	−14.978	−21.083	−20.978
(5)	0.000	0.000	−12.957	−12.845
(6)	1.056	1.057	−16.202	−16.607
(7)	13.561	13.634	1.101	1.101
(8)	11.687	11.767	0.759	0.769
(9)	−12.957	−12.845	0.720	0.731
(10)	−18.741	−18.646	1.056	1.057
(11)	0.759	0.769		
(12)	1.101	1.101		

[a] These frequencies for $\mathbf{k}=0$, which are given in units of $|J_{ad}|$, are calculated according to Eq. (29). r is the rotation eigenvalue. The modes with rotation eigenvalue λ are degenerate with those with eigenvalue λ^2 [see Eq. (13)].

[17] J. E. Robinson, Phys. Rev. **83**, 678 (1951).
[18] C. Herring and C. Kittel, Phys. Rev. **81**, 869 (1951).

IV. THE DETERMINATION OF THE EXCHANGE INTEGRALS FOR EXPERIMENTAL DATA

1. YIG

Yttrium iron garnet has been the object of several experimental studies from which information about the exchange integrals could be obtained. Using a molecular field analysis, Pauthenet[1] was able to determine values of the exchange integrals which were later apparently confirmed by high-temperature susceptibility measurements.[19] However, the values of the exchange integrals so determined give a value of 15 cm^{-1} for D [see Eq. (15)] which is in disagreement with several subsequent determinations of this quantity. For instance, by comparing the experimentally determined low-temperature specific heat[6,20–22] with the results of the spin-wave calculation, one was able to deduce that $D\approx 27$ cm^{-1}. This value of D has been corroborated by observations of the microwave instability in YIG.[23,24] Since the determination of D using a spin-wave theory is the more unambiguous both from a theoretical and an experimental standpoint, we assume it to be the more reliable. However, fixing the value of D to be 27 cm^{-1} does not serve to determine the exchange integrals uniquely since from Eq. (15) we have:

$$D=\tfrac{5}{16}(8J_{aa}-5J_{ad}+3J_{dd}). \quad (30)$$

The problem we consider is to determine values for J_{aa}, J_{dd}, and J_{ad} consistent with the known value of D and which best reproduce the detailed behavior of YIG.

Recently, Wojtowicz[25] has suggested that by taking $J_{aa}=J_{dd}=0$, one might be able to fit the susceptibility data above the Néel point using a linked cluster expansion rather than a molecular field approximation. He was able to interpret the experimental data in this way, but using a value of J_{ad} which corresponds to

[19] R. Aléonard, J. Phys. Chem. Solids **15**, 167 (1960).
[20] D. Edmonds and R. Petersen, Phys. Rev. Letters **2**, 499 (1959).
[21] J. E. Kunzler, L. R. Walker, and J. R. Galt, Phys. Rev. **119**, 1609 (1960).
[22] S. S. Shinozaki, Phys. Rev. **122**, 388 (1961).
[23] E. H. Turner, Phys. Rev. Letters **5**, 100 (1960).
[24] R. C. LeCraw and L. R. Walker, J. Appl. Phys. **32**, 167S (1961).
[25] P. J. Wojtowicz, J. Appl. Phys. **33**, 1257S (1962).

$D=38$ cm^{-1}. It is quite possible, however, that one could also fit the data using nonzero values of J_{aa} and J_{dd}, although the analysis would be formidable. In any event, exact agreement between determinations of D over widely separated temperature intervals is not to be expected, due to the sensitive dependence of the exchange integrals on the lattice constant. Also, the variation of D with temperature, as determined by microwave instability measurements, does not seem to be consistent with $J_{aa}=J_{dd}=0$, at least according to the RPA.[24]

Recently, Solt[26] has made accurate measurements of the magnetization of YIG in a magnetic field of 4000 G for temperatures between 5 and 50°K using the properties of magnetostatic modes. Since in this temperature range the magnetization varies by only 0.4%, one should check that volume changes do not influence the magnetization appreciably. In fact, using the Grüneisen relation[27] and taking the compressibility to be roughly that at room temperature as measured by Kaminow,[28] one finds the change in the magnetization due to the explicit volume dependence to be

$$\frac{\Delta M}{M}=\frac{\Delta V}{V}=\frac{\gamma\kappa}{V}\int_0^{50} C_{\text{Lattice}}dT \approx\frac{(3)(7\times10^{-13}\text{ cm}^2/\text{dyn})}{300\text{ cm}^3}(360\text{ J})\approx2.5\times10^{-5}, \quad (31)$$

where γ is the Grüneisen constant and κ the compressibility, so that the volume change is responsible for only 1% of the observed decrease in the magnetization at 50°K. (The lattice specific heat was estimated from the data of Harris and Meyer[6]). It is also known that the temperature dependence of the exchange integrals due to the change in the lattice constant in this temperature range is negligible.[29]

However, the application of an external field of even 4000 G affects the magnetization significantly at this temperatures, as we have mentioned previously. The magnetization was measured by measuring the fields for resonant excitation of the (210) and (220) magnetostatic modes at a frequency of 9092 Mc/sec. The resonance conditions are[26]

$$H_{210}=\omega/\gamma+(8\pi/15)M(H_{210}), \quad (32a)$$
$$H_{220}=\omega/\gamma-(4\pi/15)M(H_{220}), \quad (32b)$$

where $M(H)$ is the magnetization M in a field H and H_{lmn} is the field for resonance of the (lmn) magnetostatic mode. The magnetization found by subtracting the second equation from the first corresponds to an average field $\bar{H}$ for which

$$H_{210}-H_{220}=(8\pi/15)M(H_{210})+(4\pi/15)M(H_{220}) =(12\pi/15)M(\bar{H}). \quad (33)$$

Expanding $M(H_{210})$ and $M(H_{220})$ about $\bar{H}$, one finds

$$\bar{H}=\frac{H_{220}+2H_{210}}{3}=\frac{\omega}{\gamma}+\frac{4\pi}{15}M. \quad (34)$$

Anderson and Suhl[30] have found a dispersion relation for the acoustic mode taking account of dipolar interaction, which for a sphere can be written,

$$(\hbar\omega)^2=\{Da^2k^2+g\beta[H-(4\pi/3)M]\} \times\{Da^2k^2+g\beta[H-(4\pi/3)M+4\pi M\sin^2\theta_k]\}. \quad (35)$$

where θ_k is the angle between $\mathbf{k}$ and the magnetic field, $\mathbf{H}$. Since $4\pi M/3H\sim0.2$ one finds

$$\hbar\omega\approx Da^2k^2+g\beta(H-(4\pi/3)M+2\pi M\sin^2\theta_k). \quad (36)$$

For a given value of $|\mathbf{k}|$ this dispersion relation introduces a breadth of $2\pi g\beta M$ into the spectrum, but leaves the average frequency unchanged. Accordingly, the demagnetizing field can be neglected in the first approximation. In addition we have assumed that the effects of anisotropy can be taken account of by the usual anisotropy field,[31] $-4K/3M$, where K is the first-order anisotropy constant. Taking $4\pi M/5=487$ G and $K/M=-130$ G[8], we find the total field to be

$$g\beta H_{\text{tot}}=g\beta\bar{H}-\frac{4K}{3M} =\hbar\omega+\frac{4\pi}{15}g\beta M-\frac{4K}{3M}=0.309\text{ cm}^{-1}. \quad (37)$$

In order to determine $\Delta M(T)=M(0)-M(T)$ it is necessary to extrapolate $M(T)$ to $T=0$, which, however, can not be done without introducing a significant error. In the low-temperature limit $M(T)$ depends only on H_{tot} and D, which are known so that $M(0)$ could be determined by comparing the values of ΔM for temperatures below 10°K with the calculated values. The uncertainty in this procedure did not affect our determinations of the exchange integrals. We calculated the magnetization for various values of the ratios J_{aa}/J_{ad} and J_{dd}/J_{ad} the value of J_{ad} being determined to give the known value of D. By comparing the family of curves so obtained with the experimental data it was then hoped to determine J_{aa} and J_{dd}. It happened, however, that the magnetization was not sensitive to variations of the ratio J_{dd}/J_{ad}. On the other hand, the value of J_{aa}/J_{ad} did influence the calculated magneti-

[26] I. H. Solt, Jr., J. Appl. Phys. **33**, 1189S (1962); I. H. Solt, Jr. (private communication).
[27] C. Kittel, *Introduction to Solid State Physics* (John Wiley & Sons, Inc. New York, 1956), 2nd ed.
[28] I. P. Kaminow and R. V. Jones, Scientific Report No. 5 (Series 2) Gordon McKay Laboratory of Applied Science, 1960 (unpublished).
[29] I. P. Kaminow and R. V. Jones, Phys. Rev. **123**, 1122 (1961).
[30] P. W. Anderson and H. Suhl, Phys. Rev. **100**, 1788 (1955).
[31] J. Smit and H. P. J. Wijn, *Ferrites* (John Wiley & Sons, Inc., New York, 1959).

TABLE IV. Possible values of the exchange integrals in YIG and GdIG.[a]

J_{aa}/J_{ad}	J_{dd}/J_{ad}	J_{ad}	J_{aa}	J_{dd}	J_{dc}	J_{ac}
0.2	0.2	31.8	6.35	6.35	7.00	1.75
0.2	0.3	35.6	7.12	10.68	7.12	1.78
0.2	0.4	40.5	8.09	16.18	not calculated	

[a] Values of the exchange integrals are given in cm^{-1}.

zation curves, as can be seen in Fig. 15. We were thus able to deduce $J_{aa}/J_{ad}=0.2$, in contrast to the approximate analysis of Wojtowicz.[25] Considering the geometry of the garnet lattice, it would be surprising if the exchange coupling between neighboring d ions were weaker than that between neighboring a ions, since the latter are further apart than the former, so that we assume $J_{dd}\geq J_{aa}$. Since there is an optical modes whose frequency for $\mathbf{k}=0$ is $20J_{ad}-40J_{dd}$ we were able to establish the upper bound $J_{dd}\leq 0.4J_{ad}$. In Table IV we give the corresponding sets of exchange integrals together with those of GdIG whose determination is discussed below. It is hoped in the future to estimate the ratio J_{dd}/J_{ad} from the known[1] value of the Néel temperature.

2. GdIG

As we have mentioned previously, the details of the low-frequency part of the spectrum for GdIG are not very sensitive to the exact values of the iron-iron exchange integrals (assuming D to be known). We therefore, somewhat arbitrarily, made calculations taking $J_{aa}/J_{ad}=0.2$ and $J_{dd}/J_{ad}=0.2$ in the first case and $J_{dd}/J_{ad}=0.3$ in the other. The object of such calculations was to determine J_{ac} and J_{dc} separately by fitting the experimental results. Dreyfus[4] has previously determined values of J_{ac} and J_{dc} using the frequencies for $\mathbf{k}=0$ for a particular value of the ratio J_{ac}/J_{dc}. Although this procedure does not cause a great error in the determination of the exchange integrals, we thought it worthwhile to attempt such a determination taking account of the $\mathbf{k}$ dependence of the low optical modes and also seeing to what extent varying the ratio J_{ac}/J_{dc} influenced the specific heat. Above 10°K the specific heat (per unit cell) is well approximated by 24 Einstein functions appropriate to the average frequency for large values of k, since the factor k^2dk in the density of states weights the large values of k the most. This average frequency is known accurately from calorimetric measurements[6] and for a given value of J_{ac}/J_{dc} fixes the values of these exchange integrals. We then compared the experimental and theoretical values of the specific heat below 5°K for the various values of J_{ac}/J_{dc}. The results of such a procedure are shown in Fig. 16. It was found that $J_{ac}/J_{dc}=0.25$ gave the best fit to the data for both sets of values of the iron-iron exchange integrals considered. The corresponding values of J_{ac} and J_{dc} which depend slightly on the choice of the values of the iron-iron exchange integrals are given in Table IV

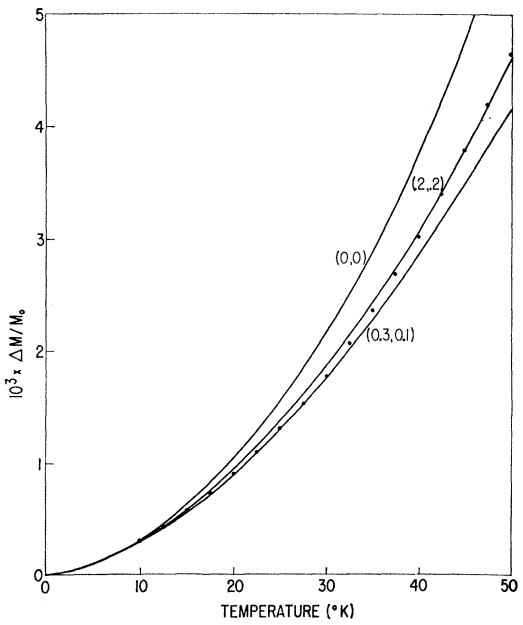

FIG. 15. The magnetization of YIG below 50°K. The dots are the experimental values of Solt (Ref. 22). The curves were calculated for the values of the ratios J_{aa}/J_{ad} and J_{dd}/J_{ad} indicated by the numbers in parentheses; the corresponding values of J_{ad} are, (0,0): $J_{ad}=17.8$ cm^{-1}, (0.3,0.1): $J_{ad}=38.0$ cm^{-1}, and (0.2,0.2): $J_{ad}=31.8$ cm^{-1}. The effective magnetic field is given by Eq. (37).

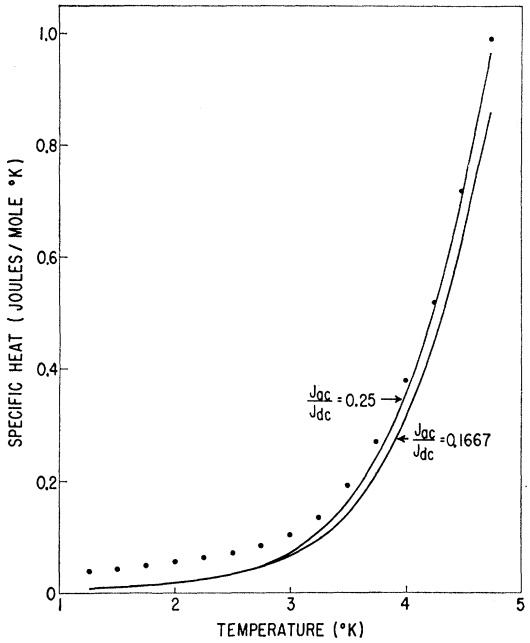

FIG. 16. The magnetic contribution to the specific heat of GdIG. The dots are the experimental values[6] and the curves are calculated taking $J_{ad}=31.8$ cm^{-1} and $J_{aa}=J_{dd}=6.35$ cm^{-1}. The values of J_{ac} and J_{dc} corresponding to the indicated values of J_{ac}/J_{dc} are, $J_{ac}/J_{dc}=0.25$: $J_{dc}=7.00$ cm^{-1} and $J_{ac}=1.75$ cm^{-1}, and $J_{ac}/J_{dc}=0.1667$: $J_{dc}=4.74$ cm^{-1} and $J_{ac}=0.79$ cm^{-1}.

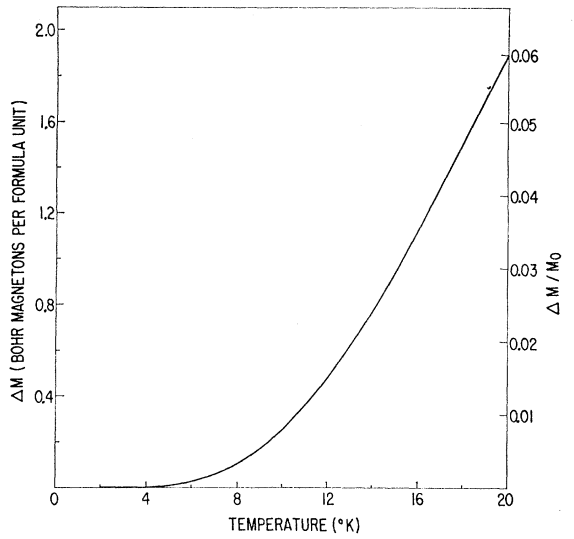

FIG. 17. The magnetization of GdIG below 20°K taking $J_{ad}=31.8$ cm^{-1}, $J_{aa}=J_{dd}=6.35$ cm^{-1}, $J_{dc}=7.00$ cm^{-1} and $J_{ac}=1.75$ cm^{-1}.

and are about 25% larger than one would expect using the WMF approximation. The reason for this can be seen from Figs. 13 and 14 where we indicate both the frequency corresponding to the WMF acting on a rare-earth ion as given by Eq. (23) and the average frequency of all the low optical modes. Equating the frequency of the single ion splitting as determined calorimetrically with the WMF frequency clearly leads to smaller values of the exchange integrals than we find. One can also compare the values of J_{ac} and J_{dc} we find with those found by Dreyfus: $J_{ac}=0.49$ cm^{-1} and $J_{dc}=4.17$ cm^{-1}. The surprising discrepancy between his values and ours is mostly due to a numerical error in his calculation of the lowest optical mode which unfortunately affects the determination of the exchange integrals rather critically.

It should be noted that we were unable to obtain a good fit to the specific heat data for temperatures below 3°K. The reason for this discrepancy is not clear at present and will be investigated experimentally in the near future. We did not attempt to obtain a better fit by altering the value of D as we did previously[6] which accounts for most of the difference between the calculations presented here and those given previously. Above 10°K the calculated and experimental values of the specific heat are in close agreement. As we show in the Appendix, one does not expect that the small temperature dependence of the frequencies of the normal modes will influence the specific heat significantly.

In Fig. 17 we show the magnetization of GdIG below 20°K as calculated for one of the sets of exchange integrals given in Table IV. The curve calculated for the other set of exchange integrals is indistinguishable from that shown. The magnetization of GdIG has been measured by Pauthenet[1] and by Wolf and Bozorth,[32] but due to experimental difficulties these measurements are not sufficiently refined to be suitable for comparison with spin-wave theory in this temperature range. No information could be obtained from the absorption spectrum of GdIG as measured by Sievers and Tinkham,[33] since the single ion transitions are forbidden in GdIG.[5]

APPENDIX

Calculation of the Zero-Point Energy

To calculate the zero-point energy we use the Holstein-Primakoff[34] expansions

$$S_i^z=S_i-a_i^+a_i^-, \tag{A1a}$$

$$S_i^+=(2S_i)^{\frac{1}{2}}a_i^-\cdots, \tag{A1b}$$

$$S_i^-=(2S_i)^{\frac{1}{2}}a_i^+\cdots, \tag{A1c}$$

for spins oriented in the plus z direction, and

$$S_i^z=-S_i+a_i^+a_i^-, \tag{A2a}$$

$$S_i^+=(2S_i)^{\frac{1}{2}}a_i^+\cdots, \tag{A2b}$$

$$S_i^-=(2S_i)^{\frac{1}{2}}a_i^-\cdots, \tag{A2c}$$

for spins oriented in the minus z direction, where $[a_i^+,a_i^-]=-1$. The Hamiltonian can be expanded as

$$\mathcal{H}=E^0+\sum_j\sum_i T_{ij}a_i^+a_j^-+\tfrac{1}{2}\sum_{ij}U_{ij}a_i^+a_j^+ +\tfrac{1}{2}\sum_{ij}U_{ij}^*a_j^-a_j^-\cdots, \tag{A3}$$

where E^0 is the expectation value of the energy in the Néel state, and $T_{ij}=T_{ji}^*$ and $U_{ij}=U_{ji}$. A more symmetric form for $\mathcal{H}$ is

$$\mathcal{H}=E_0+\tfrac{1}{2}\sum_{ij}T_{ij}(a_i^+a_j^-+a_j^-a_i^+)+\tfrac{1}{2}\sum_{ij}U_{ij}a_i^+a_j^+ +\tfrac{1}{2}\sum_{ij}U_{ij}^*a_i^-a_j^--\tfrac{1}{2}\sum_i T_{ii}. \tag{A4}$$

Thus, in this approximation the ground-state energy is different from that in the Néel state by an amount

$$\Delta E^0=-\tfrac{1}{2}\sum_i T_{ii}+\tfrac{1}{2}\sum_n|\hbar\omega_n|, \tag{A5}$$

which for a ferromagnet is zero, of course.

In the RPA one calculates the frequency spectrum at finite temperatures by substituting for S the thermal value of S_z. We now show that at low temperatures this excitation energy is not exactly what one should use in the calculation of the free energy, and that using the correct frequency one no longer need consider explicitly the zero-point energy.

[32] W. P. Wolf and R. M. Bozorth, Phys. Rev. **124**, 449 (1961).
[33] A. J. Sievers, III, and M. Tinkham, Phys. Rev. **129**, 1995 (1963).
[34] T. Holstein and H. Primakoff, Phys. Rev. **58**, 1098 (1940).

We start by assuming that the temperature is low enough so that we may write,

$$E=E^0+\Delta E^0+\sum_{\rho\mathbf{k}} n_{\rho\mathbf{k}}|\hbar\omega_{\rho\mathbf{k}}| +\tfrac{1}{2}\sum_{\rho\rho'\mathbf{k}\mathbf{k}'} n_{\rho\mathbf{k}}n_{\rho'\mathbf{k}'}V_{\rho\mathbf{k},\rho'\mathbf{k}'}. \quad \text{(A6)}$$

This formula can be made to agree with the first RPA[10] or with Dyson's[35] results with the proper choices of the coefficient, $V_{\rho\mathbf{k},\rho'\mathbf{k}'}$. From this equation one deduces an excitation energy

$$\hbar\omega_{\rho\mathbf{k}}(n_r)=\hbar\omega_{\rho\mathbf{k}}+\sum_{\rho'\mathbf{k}'} n_{\rho'\mathbf{k}'}V_{\rho\mathbf{k},\rho'\mathbf{k}'}, \quad \text{(A7)}$$

where n_r stands for the totality of occupation numbers other than $n_{\rho k}$. Using brackets, $\langle\ \rangle$, to represent thermal averages, one has

$$\hbar\omega_{\rho\mathbf{k}}(T)=\hbar\omega_{\rho\mathbf{k}}+\sum_{\rho'\mathbf{k}'} V_{\rho\mathbf{k},\rho'\mathbf{k}'}\langle n_{\rho'\mathbf{k}'}\rangle, \quad \text{(A8)}$$

where we distinguish between $\hbar\omega_{\rho\mathbf{k}}$ which is $\hbar\omega_{\rho\mathbf{k}}(T=0)$ and $\hbar\omega_{\rho\mathbf{k}}(T)$. By expanding the partition function,

$$Z=\exp[-\beta(E^0+\Delta E^0)]\sum_{\{n_{\rho k}\}}\exp\{-\beta[\sum n_{\rho\mathbf{k}}\hbar\omega_{\rho\mathbf{k}} +\tfrac{1}{2}\sum V_{\rho\mathbf{k},\rho'\mathbf{k}'}n_{\rho\mathbf{k}}n_{\rho'\mathbf{k}'}\cdots]\} \quad \text{(A9)}$$

one can write the free energy as

$$F=E^0+\Delta E^0+F(\hbar\omega_{\rho\mathbf{k}})+\tfrac{1}{2}\sum V_{\rho\mathbf{k},\rho'\mathbf{k}'}\langle n_{\rho\mathbf{k}}\rangle\langle n_{\rho\ \mathbf{k}'}\rangle, \quad \text{(A10)}$$

where $F(\hbar\omega_{\rho\mathbf{k}})$ is the free energy calculated using the zero-temperature frequencies. Since

$$\frac{\partial F}{\partial\hbar\omega_{\rho\mathbf{k}}}=k_BT\frac{\partial}{\partial\hbar\omega_{\rho\mathbf{k}}} \times\ln[1-\exp(-\hbar\omega_{\rho\mathbf{k}}/k_BT)]=\langle n_{\rho\mathbf{k}}\rangle, \quad \text{(A11)}$$

one has

$$F=E^0+\Delta E^0+F(\hbar\omega_{\rho\mathbf{k}}) +\tfrac{1}{2}\sum_{\rho\rho'\mathbf{k}\mathbf{k}'} V_{\rho\mathbf{k},\rho'\mathbf{k}'}\langle n_{\rho\mathbf{k}}\rangle(\partial F/\partial\hbar\omega_{\rho'\mathbf{k}'}), \quad \text{(A12)}$$

or using Eq. (A8)

$$F=E^0+\Delta E^0+F(\hbar\omega_{\rho\mathbf{k}})+\tfrac{1}{2}\sum_{\rho'\mathbf{k}'}[\hbar\omega_{\rho'\mathbf{k}'}(T) -\hbar\omega_{\rho'\mathbf{k}'}(0)](\partial F/\partial\hbar\omega_{\rho'\mathbf{k}'}), \quad \text{(A13)}$$

so that finally

$$F=E^0+\Delta E^0+F([\hbar\omega_{\rho\mathbf{k}}+\hbar\omega_{\rho\mathbf{k}}(T)]/2). \quad \text{(A14)}$$

Thus we see that, whereas $\hbar\omega_{\rho\mathbf{k}}(T)$ is the excitation energy one might observe in a resonance experiment, the macroscopic properties are to be calculated using the frequency $[\hbar\omega_{\rho\mathbf{k}}+\hbar\omega_{\rho\mathbf{k}}(T)]/2$.[36] These considerations are only valid as long as (A6) is a good approximation, in which case we do not expect to be able to detect the thermal variation of frequency of modes which are not excited, since the zero-point energy need not be considered explicitly. In contrast, the zero-point energy would have to be considered in cases where the external parameters upon which it depends, e.g., the magnetic field, are variable.

ACKNOWLEDGMENTS

The computations involved in this research were carried out in the Duke University Computing Laboratory which is supported in part by the National Science Foundation. The author also wishes to thank the help of the staff in carrying out the computations. The author appreciates the detailed communication of experimental data from Dr. I. H. Solt, Jr. It is a pleasure to acknowledge the stimulating discussions and advice of Professor H. Meyer during the course of this research.

[35] F. J. Dyson, Phys. Rev. **102**, 1217 (1956).

[36] F. Keffer, in *Handbuch der Physik* (to be published).